J|A|C|S
ARTICLES
Published on Web 06/30/2004

Imaging the Binding Ability of Proteins Immobilized on Surfaces with Different Orientations by Using Liquid Crystals

Yan-Yeung Luk,[†,#] Matthew L. Tingey,[†] Kimberly A. Dickson,[‡] Ronald T. Raines,[*,§,‡] and Nicholas L. Abbott[*,†]

Contribution from the Departments of Chemical and Biological Engineering, Biochemistry, and Chemistry, University of Wisconsin-Madison, Madison, Wisconsin 53706

Received November 28, 2003; E-mail: abott@engr.wisc.edu; raines@biochem.wisc.edu

Abstract: We report an investigation of the binding ability of a protein immobilized on surfaces with different orientations but in identical interfacial microenvironments. The surfaces present mixed self-assembled monolayers (SAMs) of 11-[19-carboxymethylhexa(ethylene glycol)]undecyl-1-thiol, **1**, and 11-tetra(ethylene glycol) undecyl-1-thiol, **2**. Whereas **2** is used to define an interfacial microenvironment that prevents nonspecific adsorption of proteins, **1** was activated by two different schemes to immobilize ribonuclease A (RNase A) in either a preferred orientation or random orientations. The binding of the ribonuclease inhibitor protein (RI) to RNase A on these surfaces was characterized by using ellipsometry and the orientational behavior of liquid crystals. Ellipsometric measurements indicate identical extents of immobilization of RNase A via the two schemes. Following incubation of both surfaces with RI, however, ellipsometric measurements indicate a 4-fold higher binding ability of the RNase A immobilized with a preferred orientation over RNase A immobilized with a random orientation. The higher binding ability of the oriented RNase A over the randomly oriented RNase A was also apparent in the orientational behavior of nematic liquid crystals of 4-cyano-4′-pentylcyanobiphenyl (5CB) overlayed on these surfaces. These results demonstrate that the orientations of proteins covalently immobilized in controlled interfacial microenvironments can influence the binding activities of the immobilized proteins. Results reported in this article also demonstrate that the orientational states of proteins immobilized at surfaces can be distinguished by examining the optical appearances of liquid crystals.

Introduction

The development of surface-based proteomics tools requires general and facile methods for the immobilization of proteins on surfaces in known orientations and without disruption of the protein structure. Because the number of proteins presented on a surface is small when using microarrayed protein receptors, maximization of the binding capacity of each immobilized protein molecule is central to development of sensitive protein chips.[1,2] Nonspecific adsorption of nontargeted proteins must also be minimized. Many approaches leading to the immobilization of proteins, such as via imine formation between the lysine side chains of a protein and aldehyde-modified glass slides, result in the decoration of surfaces with proteins without control of their orientations.[3,4] The presentation of protein receptors with multiple orientations can be useful when the binding domain within the protein is unknown.[5,6] In contrast, when the location of the binding domain of a protein is known, the oriented immobilization of proteins is generally thought to be preferable.[7,8] This notion has motivated several approaches leading to the oriented immobilization of proteins on surfaces, including the use of protein A (to bind the Fc region of an antibody),[9,10] the immobilization of oriented Fab′ fragment of antibodies,[11] the use of fusion proteins with oligohistidine[12] or cutinase domains,[13] as well as the use of affinity contact printing.[14]

A major challenge underlying the use of immobilized proteins is preserving the binding/catalytic activities of the proteins. Various factors can lead to loss of activity, including confor-

* To whom correspondence may be addressed: abbott@engr.wisc.edu or raines@biochem.wisc.edu.
[†] Department of Chemical & Biological Engineering.
[‡] Department of Biochemistry.
[§] Department of Chemistry.
[#] Current address: Department of Chemistry, Syracuse University, Syracuse, NY 13244.

(1) Kodadek, T. *Trends Biochem. Sci.* **2002**, *27*, 295.
(2) Kodadek, T. *Chem. Biol.* **2001**, *8*, 105.
(3) Huang, S. C.; Caldwell, K. D.; Lin, J. N.; Wang, H. K.; Herron, J. N. *Langmuir* **1996**, *12*, 4292.
(4) Nakanishi, K.; Muguruma, H.; Karube, I. *Anal. Chem.* **1996**, *68*, 1695.
(5) MacBeath, G.; Schreiber, S. L. *Science* **2000**, *289*, 1760.
(6) MacBeath, G.; Koehler, A. N.; Schreiber, S. L. *J. Am. Chem. Soc.* **1999**, *121*, 7967.
(7) Huang, W.; Wang, J. Q.; Bhattacharyya, D.; Bachas, L. G. *Anal. Chem.* **1997**, *69*, 4601.
(8) Lee, Y. S.; Mrksich, M. *Trends Biotechnol.* **2002**, *20*, S14.
(9) Van Oss, C. J.; Van Regenmortel, M. H. V. *Immunochemistry*; Dekker: New York, 1994.
(10) Turkova, J. *J. Chromatogr., B* **1999**, *722*, 11.
(11) Spitznagel, T. M.; Jacobs, J. W.; Clark, D. S. *Enzyme Microb. Technol.* **1993**, *15*, 916.
(12) Zhu, H.; Bilgin, M.; Bangham, R.; Hall, D.; Casamayor, A.; Bertone, P.; Lan, N.; Jansen, R.; Bidlingmaier, S.; Houfek, T.; Mitchell, T.; Miller, P.; Dean, R. A.; Gerstein, M.; Snyder, M. *Science* **2001**, *293*, 2101.
(13) Hodneland, C. D.; Lee, Y. S.; Min, D. H.; Mrksich, M. *Proc. Natl. Acad. Sci. U.S.A.* **2002**, *99*, 5048.
(14) Renault, J. P.; Bernard, A.; Juncker, D.; Michel, B.; Bosshard, H. R.; Delamarche, E. *Angew. Chem., Int. Ed.* **2002**, *41*, 2320.

10.1021/ja0398565 CCC: $27.50

mational changes (partial denaturation) induced by immobilization, and immobilization in orientations that bury the active site. The microenvironment of the interface can also influence the activity of immobilized proteins. For example, surface charge density can influence the approach of binding partners from bulk solution, solvent structure at the interface can affect the binding activities, and nonspecific protein adsorption or protein−protein association can occur when the density of the immobilized protein is high.[8,11] Hence, lack of control over surface chemistry in general leads to interfacial microenvironments that can compromise the activity of immobilized proteins.[8]

Because of these issues, past studies have not provided unambiguous evidence of the influence of protein orientation on the binding ability of proteins immobilized on surfaces.[15−21] For examples, Saavedra and co-workers illustrated the importance of controlling interfacial microenvironments when developing approaches for oriented immobilization of proteins.[15−19] By immobilizing cyt *c* with a monomeric cysteine residue on a thiol-capped silane monolayer, the authors found a broad distribution of orientations of the heme groups in cyt *c* due to nonspecific adsorption of cyt *c* on the thiol-capped surface.[17] Similarly, immobilization of cyt *c* to a pyridyl disulfide-capped phospholipid bilayer on a glass substrate via a disulfide bond afforded 70% oriented cyt *c* (due to disulfide linkage) and 30% nonspecifically adsorbed cyt *c* on these surfaces.[18] Interestingly, a recent study also by Saavedra and co-worker demonstrated that electrostatically driven adsorption of positively charged cyt *c* (horse heart cytochrome *c*) on a negatively charged (sulfonate) silane-based SAM produced narrower distribution of orientations of cyt *c* than site-directed covalent immobilization (disulfide formation) of cyt *c* that is accompanied by nonspecific adsorption.[16] These results demonstrate the importance of controlling nonspecific adsorption of proteins when covalent attachment is employed to achieve oriented immobilization of proteins. Leckband and co-workers have also reported studies of the influence of interfacial microenvironment on the covalent immobilization of proteins.[20,21] A variant of cytochrome b_5 (T8C) that possessed a monomeric cysteine was covalently coupled to the maleimide groups of supported lipid bilayers (using a linker that was either neutral or negatively charged) to afford covalent immobilization of cyt b_5 on the bilayers. The authors found that the surface coverage of covalently immobilized cyt b_5 was significantly higher on the neutral surfaces than the negatively charged surfaces.[21] This work illustrates how changes in microenvironment of an interface presenting the same reactive group can influence the extent of immobilization of proteins. These authors also compared the binding of cyt *c* to cyt b_5 immobilized with two different orientations.[20] Two different variants of cyt b_5 (T8C and T65C) biotinylated on installed cysteine residues (8 and 65) were immobilized onto a monolayer of streptavidin-tethered lipids to afford different orientations of cyt b_5. The authors did not observe a measurable difference in the binding between cyt *c* and the two variants of cyt b_5. The authors attributed this observation to the dynamic nature of the cyt *c*−cyt b_5 complex and to similar binding site accessibility of both orientations of cyt b_5.[20]

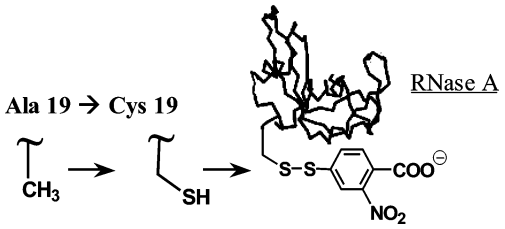

Figure 1. Schematic illustration of the preparation of the A19C variant of RNase A. Residue 19 (alanine) is replaced with a cysteine, which is subsequently protected by reaction with DTNB.

In this article, we report the results of an experimental system that permits the unambiguous identification of the influence of the orientation of an immobilized protein on its binding ability. To compare the binding ability of proteins on surfaces with either random or preferred orientation, we designed an experimental system that satisfied three criteria. First, the surfaces prevented nonspecific protein adsorption, thus leading to the exclusive immobilization of protein via a covalent linkage. Second, the areal density of protein molecules on the surface was designed to be constant, independent of the mode of immobilization (random or oriented). Third, the system permitted the immobilization of proteins in different orientations but identical interfacial microenvironment so as to minimize the influence of confounding factors (e.g., variation in solvent structure) on the binding ability of the immobilized proteins.

Our studies are based on immobilization of ribonuclease A (RNase A, 13.7 kDa). Recent studies of RNase A have revealed biological functions that include antitumor, immunosuppressive, embryotoxic, and aspermatogenic activities.[22−24] In this article, we report the binding ability of immobilized RNase A with its most potent known inhibitor: the ribonuclease inhibitor protein (RI, 50 kDa). The K_d for the RI·RNase A complex has been measured to be in the femtomolar range (4.4×10^{-14} to 6.7×10^{-14} M).[25,26] To immobilize RNase A on a surface with controlled orientation and without interfering with the binding site of RNase A for RI, we prepared a RNase A variant in which alanine 19 was replaced by a cysteine protected as a mixed disulfide with 2-nitro-5-thiobenzoic acid (NTB) (Figure 1).[27,28] Alanine 19 was chosen because it is in a solvent-exposed loop that is not in the RI·RNase A binding interface.

We prepared surfaces for immobilization of RNase A by forming mixed self-assembled monolayers (SAMS) from alkanethiols **1** and **2** on evaporated films of gold.

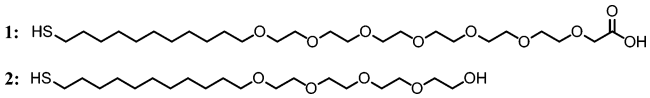

Whereas the ethylene glycol moieties provide a molecularly

(15) Edmiston, P. L.; Lee, J. E.; Cheng, S. S.; Saavedra, S. S. *J. Am. Chem. Soc.* **1997**, *119*, 560.
(16) Du, Y. Z.; Saavedra, S. S. *Langmuir* **2003**, *19*, 6443.
(17) Wood, L. L.; Cheng, S. S.; Edmiston, P. L.; Saavedra, S. S. *J. Am. Chem. Soc.* **1997**, *119*, 571.
(18) Edmiston, P. L.; Saavedra, S. S. *Biophys. J.* **1998**, *74*, 999.
(19) Edmiston, P. L.; Saavedra, S. S. *J. Am. Chem. Soc.* **1998**, *120*, 1665.
(20) Yeung, C.; Purves, T.; Kloss, A. A.; Kuhl, T. L.; Sligar, S.; Leckband, D. *Langmuir* **1999**, *15*, 6829.
(21) Yeung, C.; Leckband, D. *Langmuir* **1997**, *13*, 6746.
(22) Raines, R. T. *Chem. Rev.* **1998**, *98*, 1045.
(23) Leland, P. A.; Raines, R. T. *Chem. Biol.* **2001**, *8*, 405.
(24) Leland, P. A.; Staniszewski, K. E.; Kim, B. M.; Raines, R. T. *J. Biol. Chem.* **2001**, *276*, 43095.
(25) Lee, F. S.; Shapiro, R.; Vallee, B. L. *Biochemistry* **1989**, *28*, 225.
(26) Vicentini, A. M.; Kieffer, B.; Matthies, R.; Meyhack, B.; Hemmings, B. A.; Stone, S. R.; Hofsteenge, J. *Biochemistry* **1990**, *29*, 8827.
(27) Kothandaraman, S.; Hebert, M. C.; Raines, R. T.; Nibert, M. L. *Virology* **1998**, *251*, 264.
(28) Sweeney, R. Y.; Kelemen, B. R.; Woycechowsky, K. J.; Raines, R. T. *Anal. Biochem.* **2000**, *286*, 312.

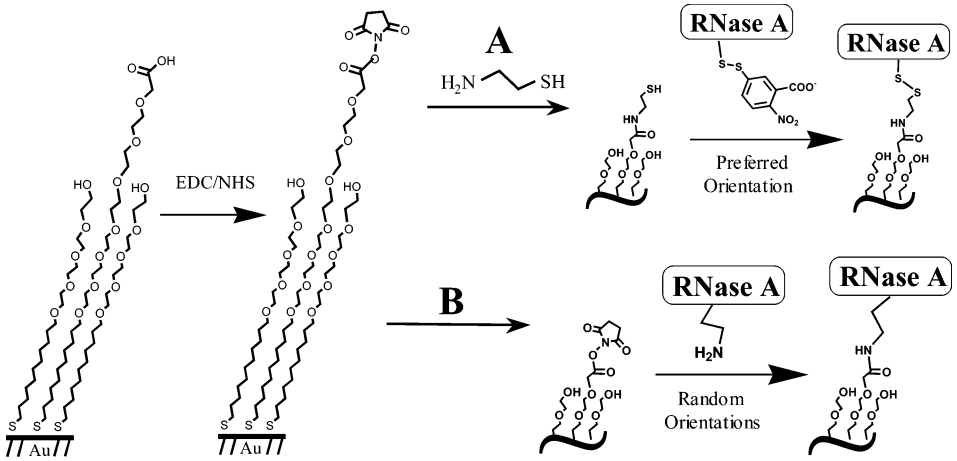

Figure 2. A SAM presenting a mixture of carboxylic acid groups and tetra(ethylene glycol) groups is activated by EDC/NHS to form a monolayer presenting an NHS ester. RNase A is immobilized via the activated SAMs with either a unique orientation (A) or random orientations (B). (A) The NHS-activated SAMs are coupled with 2-aminoethanethiol to present thiol groups on the surface. The thiol groups selectively couple with the NTB-protected cysteine residue of A19C RNase A, forming a covalent disulfide bond to afford RNase A immobilized with a unique orientation. (B) The amino groups of lysine residues and N-terminus of the wild-type RNase A directly couple to the NHS-activated acid on SAMs to afford immobilized RNase A without a unique orientation.

defined interface that is known to resist nonspecific adsorption of proteins,[29,30] the carboxylic acids are activated in our scheme to facilitate two different modes of protein immobilization. In one scheme, we use a chemoselective coupling[28] between a thiol group presented by the surface and an activated cysteine[31,32] in RNase A (Figure 2A). In a second scheme, the NHS-activated SAMs are directly treated with wild-type RNase A. The lysine residues in the RNase A directly couple with the NHS ester presented by these surfaces to afford another type of covalent immobilization of RNase A (Figure 2B). Because the coupling of the surface thiol groups to the A19C RNase A is selective, the A19C RNase A immobilized on the thiol-terminated SAMs should assume a preferred orientation. In contrast, because each RNase A molecule presents 10 lysine residues and an N-terminal amino group, immobilization of wild-type RNase A on the NHS-activated surface should afford RNase A with random orientations. Although the kinetics of the two different immobilization schemes (Figure 2A,B) are not designed to be identical, the areal densities of immobilized protein that result from the two immobilization schemes are controlled by the areal density of reactive sites on the surfaces as the reactions are driven to completion (see below).

We assess the binding ability of RNase A immobilized with the schemes shown in Figure 2 by using ellipsometry and the orientational behavior of liquid crystals.[33−35] Measurements of ellipsometric thickness following each binding event provide an optical thickness of the layer of protein bound on the surface.[36] This optical thickness is similar to that measured by using surface plasmon reflectometry.[37] The orientational behavior of liquid crystals on surfaces can also be used to report the presence of proteins bound to surfaces.[33−36] In contrast to ellipsometric measurements, however, the orientations of liquid crystals are sensitive to the structure and organization of molecules immobilized on surfaces.[38] In this article, we report experimental results that demonstrate that the orientational states of proteins immobilized at surfaces can be distinguished by examining the optical appearances of liquid crystals.

Experimental Section

Materials. The glass microscope slides were Fisher's Finest, premium grade obtained from Fisher Scientific (Pittsburgh, PA). The nematic liquid crystal 4-cyano-4′-pentylbiphenyl (5CB), manufactured by BDH, was purchased from EMD Chemicals (Hawthorne, NY). All other chemicals were obtained from Aldrich Chemicals (Milwaukee, WI) and used as received.

Preparation of A19C RNase A and Ribonuclease Inhibitor. An RNase A variant in which alanine 19 is replaced with a cysteine residue was produced using a published procedure and then protected by reaction with 5,5′-dithiobis(2-nitrobenzoic acid) (DTNB).[28] The A19C RNase A was purified by a Mono S cation-exchange FPLC column (Pharmacia, Piscataway, NJ) to ensure the purity of final product (data not shown). RI was produced using a published procedure.[39] Wild-type RNase A (type I-A from bovine pancreas) was from Sigma Chemical (St. Louis, MO) and was used without further purification.

Cleaning of Substrates. Microscope slides were cleaned sequentially in piranha (70% H_2SO_4, 30% H_2O_2) and base solutions (70% KOH, 30% H_2O_2), using nitrogen to provide agitation (1 h at ∼80 °C). *Warning: Piranha solution should be handled with extreme caution; in some circumstances, most probably when it has been mixed with significant quantities of an oxidizable organic material, it has detonated unexpectedly.* The slides were then rinsed thoroughly in deionized water (18.2 MΩ-cm), ethanol, and methanol and dried under a stream of N_2-(g). The clean slides were stored in a vacuum oven at 110 °C. All other glassware was cleaned in piranha solution prior to use.

Uniform Deposition of Gold Films. Semi-transparent films of gold with thicknesses of ∼100 nm were deposited onto glass slides mounted on rotating planetaries (no preferred direction or angle of incidence) by using an electron beam evaporator (VES-3000-C manufactured by Tek-Vac Industries, Brentwood, NY). The rotation of the substrates on the planetaries ensured that the gold was deposited without a

(29) Prime, K. L.; Whitesides, G. M. *Science* **1991**, *252*, 1164.
(30) Prime, K. L.; Whitesides, G. M. *J. Am. Chem. Soc.* **1993**, *115*, 10714.
(31) Drewes, G.; Faulstich, H. *Anal. Biochem.* **1990**, *29*, 109.
(32) Ellman, G. L. *Arch. Biochem. Biophys.* **1959**, *82*, 70.
(33) Gupta, V. K.; Skaife, J. J.; Dubrovsky, T. B.; Abbott, N. L. *Science* **1998**, *279*, 2077.
(34) Skaife, J. J.; Abbott, N. L. *Langmuir* **2000**, *16*, 3529.
(35) Skaife, J. J.; Brake, J. M.; Abbott, N. L. *Langmuir* **2001**, *17*, 5448.
(36) Luk, Y. Y.; Tingey, M. L.; Hall, D. J.; Israel, B. A.; Murphy, C. J.; Bertics, P. J.; Abbott, N. L. *Langmuir* **2003**, *19*, 1671.
(37) Mrksich, M.; Sigal, G. B.; Whitesides, G. M. *Langmuir* **1995**, *11*, 4383.
(38) Luk, Y. Y.; Abbott, N. L. *Science* **2003**, *301*, 623.
(39) Klink, T. A.; Vicentini, A. M.; Hofsteenge, J.; Raines, R. T. *Protein Expression Purif.* **2001**, *22*, 174.

Scheme 1

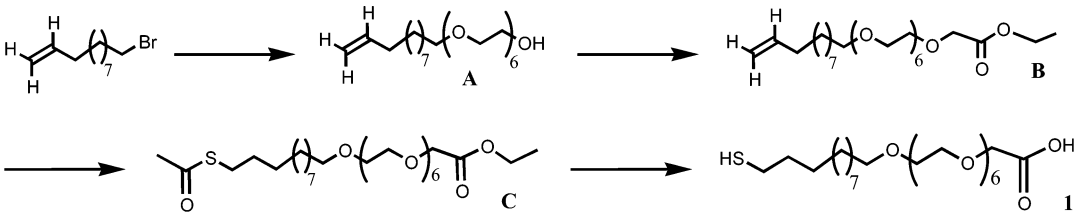

preferred direction of incidence. We refer to these gold films as "uniformly deposited gold films". A layer of titanium (thickness ~10 nm) was used to promote adhesion between the glass microscope slide and the film of gold. The rates of deposition of gold and titanium were ~0.2 Å/s. The pressure in the evaporator was less than 5×10^{-7} Torr before and during each deposition. The gold source was periodically cleaned by sequentially immersing it in aqua regia (70% HNO_3, 30% HCl) and piranha solutions at 50 °C (30 min in each solution). The cycle was repeated 3 to 4 times, rinsing between cycles in deionized water.

Oblique Deposition of Gold Films. Semi-transparent films of gold with thicknesses of ~13 nm were deposited onto glass microscope slides mounted on stationary holders by using the electron beam evaporator described above. The gold was deposited from a fixed direction of incidence and a fixed angle of incidence of 40° (measured from the normal of the surface). We refer to these gold films as "obliquely deposited gold films". A layer of titanium (thickness of ~5 nm) was used to promote adhesion between the glass and the film of gold.

Synthesis of Alkanethiols 1 and 2. The hexa(ethylene glycol)-terminated alkanethiol (**2**) was synthesized using published procedures.[40] The carboxylic acid-terminated alkanethiol (**1**) was synthesized by four steps (Scheme 1) using published procedures.[40−42]

11-Hexa(ethylene glycol)-1-undecene (A). 11-Bromo-1-undecene was added to a solution of containing excess hexa(ethylene glycol) (neat, 20 equiv) and NaOH (50 wt %, 1 equiv) over 5 min. After being stirred at 70 °C for 12 h, the solution was mixed with hexane and water and neutralized with HCl (1 N). The aqueous phase was then extracted six times with hexane; the combined organic extracts were dried over $MgSO_4$, concentrated in vacuo, and purified by flash chromatography (ethyl acetate) to give olefin **A** as a clear oil. ^{1}H NMR (250 MHz, $CDCl_3$): δ 1.26−1.29 (br s, 12H), 1.53−1.58 (qui, 2H), 2.00−2.04 (dd, 2H, J = 7.02, 6.77 Hz), 3.43 (t, 2H, J = 6.79 Hz), 3.57−3.76 (m, 24H), 4.88−4.96 (m, 2H), 5.74−5.84 (m, 1H). ESI calcd for $[MNa]^+$, 457.3244; found, 457.2.

Undecenyl 11-Hexa(ethylene glycol) Acetic Acid Ethyl Ester (B). A solution of 11-hexa(ethylene glycol)-1-undecene **A** (0.83 g, 1.912 mmol) in dry dichloromethane (20 mL) was stirred at 0 °C for 10 min, followed by addition of ethyl diazoacetate (0.48 mL, 3.824 mmol) and BF_3·Et_2O (20 μL, 0.1912 mmol). After the mixture was stirred for 30 min at 0 °C, saturated aqueous ammonium chloride (10 mL) was added, and the reaction mixture was placed in a separatory funnel. The organic phase was collected, and the aqueous phase was extracted with dichloromethane (5 × 30 mL). The combined organic phases were dried over $MgSO_4$ and concentrated in vacuo to give yellow oil. Purification by flash chromatography using gradient elution (1:1 ethyl acetate/hexane → ethyl acetate) gave 783 mg (2.018 mmol, 60%) of ester **B** as a clear oil. ^{1}H NMR (250 MHz, $CDCl_3$): δ 1.29−1.33 (m, 15H), 1.53−1.58 (m, 2H), 2.00−2.04 (dd, 2H, J = 7.02, 6.77 Hz), 3.43 (t, 2H, J = 6.79 Hz), 3.49−3.76 (m, 24H), 4.13 (s, 2H), 4.20 (q, 2H, J = 7.14 Hz), 4.88−4.96 (m, 2H), 5.74−5.84 (m, 1H).

Thioacetate C. A solution of olefin **B** (0.73 g, 1.402 mmol) in dry THF (20 mL) containing thioacetic acid (0.13 mL, 1.96 mmol) and AIBN (13 mg, 0.077 mmol) was irradiated in a photochemical reactor (Rayonet reactor lamp, Southern New England Ultraviolet Co., model no. RPR-100) for 5 h under in nitrogen (ca. 1 atm). Concentration of the reaction mixture in vacuo, followed by flash chromatography (30:1 CH_2Cl_2/MeOH) gave compound **C** as a clear oil (0.84 g, 1.304 mmol, 93%). ^{1}H NMR (250 MHz, $CDCl_3$): δ 1.29−1.33 (m, 17H), 1.53−1.58 (m, 2H), 2.00−2.04 (dd, 2H, J = 7.02, 6.77 Hz), 2.3 (s, 3H), 2.8 (t, 2H), 3.43 (t, 2H, J = 6.79 Hz), 3.49−3.76 (m, 24H), 4.13 (s, 2H), 4.20 (q, 2H, J = 7.14 Hz).

11-Mercapto-undecyl-hexa(ethylene glycol) Acetic Acid (1). A solution of thioacetate **C** (100 mg, 0.17 mmol) in MeOH (5 mL) and a solution of NaOH (50 wt %, 1 equiv) were mixed together and stirred under argon for 5 h at room temperature. Acetic acid was then added to neutralize the reaction mixture. The residue product was concentrated in vacuo to give thiol **1**. ^{1}H NMR (250 MHz, $CDCl_3$): δ 1.29−1.33 (m, 16H), 1.53−1.59 (m, 2H), 2.55 (t, 2H), 3.43 (t, 2H, J = 6.79 Hz), 3.49−3.76 (m, 24H), 4.13 (s, 2H). ESI calcd for $[MNa]^+$, 549.3176; found, 549.2.

Preparation of Optical Cells for Surface Imaging Using Liquid Crystals. Optical cells were fabricated from two films of gold, each of which supported mixed SAMs that had been incubated with the proteins of interest.[33−36] The two gold films (obliquely deposited at 40° from normal of the surface) were aligned facing each other, with the direction of deposition of each gold film parallel to the other. The gold films were then clipped together (binder or bulldog clips) using a thin film of Mylar or Saran Wrap (nominal thickness ~13 μm) to space the two surfaces apart. A drop of 5CB heated into its isotropic phase (33 °C < T < 45 °C) was then drawn by capillarity into the cavity between the two surfaces of the optical cell. The cell was subsequently cooled to room temperature, and the optical texture was observed with an Olympus BX-60 polarizing light microscope (Tokyo, Japan) in transmission mode.

Activation of SAMs and Binding of Proteins on SAMs. The kinetics of the reactions that underlie the two immobilization schemes reported in this article are expected to be different. Thus, to achieve comparable surface area coverages of immobilized proteins via the two schemes, we used reaction times and reagent concentrations that were determined to drive each immobilization reaction on the surface to completion. Procedures for activation of the carboxylic acids on SAMs to afford NHS esters were adopted and modified from published procedures.[41] Briefly, SAMs formed from solutions of 45% **1** and 55% **2** (mole ratio; total concentration 1 mM in ethanol) were soaked in solutions of EDC/NHS (200 mM/50 mM in 50/50 H_2O/DMF) for 40 min. For immobilization of RNase A with preferred orientation (Figure 2A), the NHS-activated carboxylic acid-terminated SAMs were directly transferred to a solution of 200 mM of 2-aminoethanethiol and 20 mM of diisopropylethylamine for 20 min. The substrates were then rinsed with ethanol and dried under a stream of nitrogen and incubated in a phosphate-buffered saline (PBS) containing A19C RNase A (1 μM, pH 7.4) for 4 h. For immobilization of RNase A with random orientations (Figure 2B), the NHS-activated SAMs were rinsed briefly with PBS containing wild-type RNase A (1 μM, pH 8.5) and then incubated in the PBS containing wild-type RNase A for 4 h. Binding of RI to surface-bound RNase A (with either mode of immobilization) was also carried out by using procedures similar to those previously published.[41] Briefly, immobilized RNase A was incubated in a Tris

(40) Palegrosdemange, C.; Simon, E. S.; Prime, K. L.; Whitesides, G. M. *J. Am. Chem. Soc.* **1991**, *113*, 12.
(41) Lahiri, J.; Isaacs, L.; Grzybowski, B.; Carbeck, J. D.; Whitesides, G. M. *Langmuir* **1999**, *15*, 7186.
(42) Houseman, B. T.; Mrksich, M. *J. Org. Chem.* **1998**, *63*, 7552.

Table 1. Ellipsometric Thickness (nm) and Wettability of SAMs Presenting Thiol Groups Before and After Treatment with Hexadecanethiol (HDT)

	% of **1**[a]	thickness[b]	Δ thickness[b]	wet by H_2O
before treatment[c]	37	2.4 ± 0.1		yes
	46	2.5 ± 0.1		yes
after treatment	37	3.4 ± 0.1	1 ± 0.1	no
	46	4.0 ± 0.1	1.5 ± 0.1	no

[a] Percent of alkanethiol **1** in ethanolic solution. [b] In nanometers. [c] Treatment: Activation with NHS/AET and reaction with hexadecanethiol.

buffer containing RI (1 μM, pH 7.4, 2 mM Tris, 10 mM EDTA, 100 mM NaCl, 10 mM DTT) for 30 min.

Ellipsometry. Ellipsometric measurements were performed to determine the optical thicknesses of SAMs and films of proteins. The reported optical thickness of each sample is the average of 4 to 5 measurements performed at different locations on each substrate by using a Rudolph Auto EL ellipsometer (Flanders, NJ) at a wavelength of 632 nm and an angle of incidence of 70°. The gold substrates used for ellipsometric measurements were 100 nm in thickness (Au) and were deposited without a preferred direction or angle of incidence. The ellipsometric thicknesses of SAMs and immobilized proteins were estimated by using a three-layer model and by assuming a refractive index of 1.46 for both the monolayer and protein.

Results and Discussion

Whereas the coupling of lysine groups of a protein to NHS-activated carboxylic acid groups on SAMs (Figure 2B) is well-documented,[41] the reaction between NTB-protected cysteine groups of a protein and thiol groups of SAMs (Figure 2A) has not been reported. Therefore, we first evaluated the reactivity of the thiol groups on surfaces prepared by coupling of 2-aminoethanethiol ($H_2NCH_2CH_2SH$) to NHS-activated carboxylic acid groups of SAMs. After treating the NHS-activated carboxylic acid-terminated SAMs with $H_2NCH_2CH_2SH$ (see Experimental Section), the SAMs were soaked in a solution of hexadecanethiol (2 mM) and hydrogen peroxide (~1μL/3 mL) in ethanol for 30 min. The changes in ellipsometric thickness and wettability by water are tabulated in Table 1.

Inspection of Table 1 reveals that treatment of the SAMs with hexadecanethiol transforms the surface from one wet by water to one that is not. Furthermore, reaction of SAMs prepared from 37% of **1** and 63% of **2** with hexadecanethiol caused the ellipsometric thickness to increase by 1 ± 0.1 nm, whereas reaction of SAMs prepared from 46% of **1** and 54% of **2** with hexadecanethiol caused the ellipsometric thickness to increase by 1.5 ± 0.1 nm. This increase in ellipsometric thickness of the monolayer upon reaction with HDT correlates with the surface density of alkanethiol **1**. These results, when combined with the increase in the hydrophobicity of the SAMs after treatment with hexadecanethiol, indicate that the thiol groups on the surface are reactive and the extent of incorporation of HDT is controlled by the density of reactive groups.

Next, we investigated the immobilization of A19C RNase A on thiol-terminated SAMs with different surface densities of alkanethiol **1** (Figure 2A). We note that while a native cysteine in a protein could be used for site-specific immobilization via disulfide formation with ligands presented on a surface,[17] the free thiol group in the protein can cause protein dimerization by forming disulfide bonds between protein molecules. Hence, we have used NTB-protected thiol groups as activated cysteines to prevent dimerization of the protein. The NTB groups on cysteines are good leaving groups for disulfide exchange with the free thiol groups presented on the surface. We examined

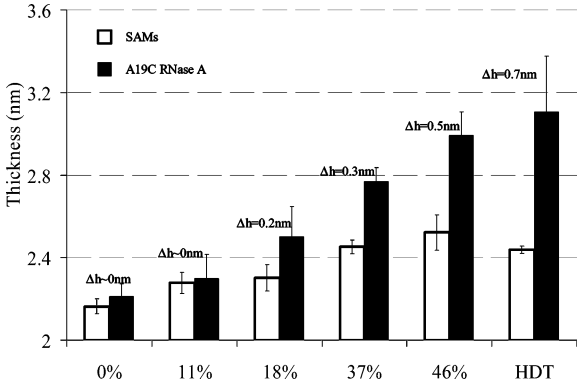

Figure 3. Average ellipsometric thicknesses of SAMs prepared from either mixtures of alkanethiols **1** and **2** dissolved in ethanol or hexadecanethiol (white bars), and average ellipsometric thicknesses of these surfaces after activation of the acid groups of **1** by 3-aminoethanethiol ($H_2NCH_2CH_2SH$) and treatment with A19C RNase A (black bars). The composition of the solution (percent alkanethiol **1**) is indicated on the *x*-axis. HDT denotes SAMs prepared from hexadecanethiol.

the immobilization of A19C RNase A (1 μM in PBS) on thiol-terminated SAMs by ellipsometry using incubation times of 30 min, 1 h, and 4 h. We measured the ellipsometric thickness of captured protein to be constant for incubation times greater than 30 min, consistent with a maximization of the extent of reaction on the surface. To ensure maximal reaction of the thiol-terminated SAMs, we used an incubation time of 4 h for the remainder of the experiments reported in this article.

Figure 3 shows the ellipsometric thicknesses of SAMs prepared from various mixtures of **1** and **2** before and after activation of the acid groups with 3-aminoethanethiol ($H_2NCH_2CH_2SH$) and treatment with the A19C RNase A. For the purpose of comparison, results obtained with SAMs formed from hexadecanethiol are also shown. Inspection of Figure 3 reveals that the ellipsometric thickness of the SAMs increases with the ratio of alkanethiol **1** to alkanethiol **2** in solution, indicating an increase in the surface density of the longer alkanethiol **1**. Treatment of the mixed SAMs with A19C RNase A causes an increase in the measured thickness. The increment of the ellipsometric thickness after treatment of A19C RNase A also increases with the percentage of alkanethiol **1**, consistent with a specific coupling between the A19C RNase A and the thiol groups on SAMs (see below for additional evidence for specific coupling). We note that the increment in ellipsometric thickness of RNase A physically adsorbed on a hydrophobic surface, a SAM prepared from form hexadecanethiol (HDT), is larger than the increment of RNase A specifically immobilized on mixed SAMs with low surface density of thiol-terminated alkanethiols (by using low ratio of alkanethiols **1**/**2** in the ethanolic solution). This result supports the proposition that the density of reactive groups presented by these mixed SAMs controls the amount of RNase A immobilized on the mixed SAMs.

Next, we investigated the selectivity of the immobilization of A19C RNase A on thiol-terminated SAMs (Figure 2A). Figure 4 shows a comparison of ellipsometric thicknesses resulting from the immobilization of wild-type and A19C RNase A on thiol-terminated SAMs (Figure 2A) and methyl-terminated SAMs ($CH_3(CH_2)_{15}SH$). Inspection of Figure 4 reveals that while treatment of SAMs presenting thiol groups with A19C RNase A caused an increase in the ellipsometric thickness of 0.5 ± 0.1 nm, treatment of wild-type RNase A did not cause a measurable increase in the ellipsometric thickness of these interfaces. In contrast, on SAMs formed from hexadecanethiol,

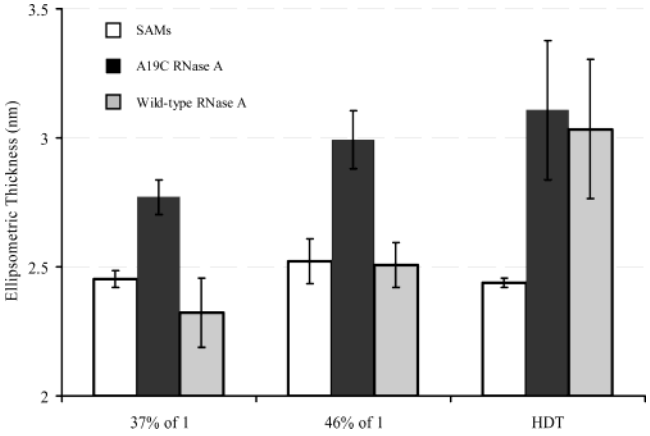

Figure 4. Selectivity of the immobilization of A19C RNase A and wild-type RNase A on thiol-terminated SAMs. Average ellipsometric thickness of mixed SAMs prepared from **1** and **2** and hexadecanethiols (HDT) (white bars), average ellipsometric thickness of SAMs activated by $H_2NCH_2CH_2$-SH and treated with A19C RNase A (black bars) and wild-type RNase A (gray bars).

treatment of both wild-type and A19C RNase A led to the same increase in ellipsometric thickness (0.7 nm). There are no free thiol groups in the native RNase A. Native RNase A does contain four disulfide bonds formed from the thiols of its eight cysteine residues. The disulfide bonds are highly stable and contribute to the robustness of RNase A.[43] The only free thiol group in the mutant RNase A (A19C RNase A) is due to the introduction of the cysteine residue at position 19. Therefore, these results indicate that the immobilization of RNase A on the thiol-terminated SAMs is highly selective to the presence of the site-directed incorporation of an activated cysteine group (i.e., NTB-protected cysteine in A19C RNase A) and that the surfaces resist nonspecific adsorption of RNase A.

Immobilization of wild-type RNase A on SAMs presenting NHS-activated carboxylic acids (Figure 2B) was carried out with procedures similar to that previously published for other proteins.[41] The 10 lysine residues in RNase A are uniformly distributed along the primary sequence of the protein (appearing at positions 1, 7, 31, 37, 41, 61, 66, 91, 98, and 104 of the 124-residue sequence).[22] When reacted with NHS-activated carboxylic acid groups, these lysine residues should cause the immobilized RNase A to assume an ensemble of up to 10 different orientations on the surface. A 4-h incubation of wild-type RNase A on NHS-activated SAMs (formed from 46% of **1** and 54% of **2**) afforded a layer of protein with the same optical thickness (0.5 ± 0.1 nm) as that obtained by immobilization of A19C RNase A on the thiol-terminated SAMs (Table 2). These results indicate that the two different schemes of immobilization reported herein can be used to immobilize the same amount of wild-type and A19C RNase A on SAMs.

Next, we investigated the binding of RI to RNase A immobilized on SAMs via the two schemes shown in Figure 2. Ellipsometric measurements indicated an increase in thickness of 1.7 ± 0.4 nm upon binding of RI to A19C RNase A immobilized on the thiol-terminated SAMs. Treatment of immobilized A19C RNase A with BSA or the RI·RNase A complex did not cause a significant increase in ellipsometric thickness. In contrast, binding of RI to wild-type RNase A immobilized on the NHS ester-terminated SAM caused an increase in ellipsometric thickness of only 0.4 ± 0.4 nm. Control experiments in which the immobilized wild-type RNase A was treated with either BSA or the RI·RNase A complex did not afford any significant increase in ellipsometric thickness of the interfacial layer (Table 2).

A past study by de Feijter and co-workers has derived the relationship between the ellipsometric thickness and mass per unit area of protein immobilized on surface to be[44]

$$\Gamma = <h_1>(<n_1> - n_2)/(\mathrm{dn/dc})$$

where Γ is the mass of protein per unit area, $<h_1>$ is the average ellipsometric thickness of the protein layer, $<n_1>$ is the average refractive index of the protein layer (1.46), n_2 is the refractive index of air (1.00), and dn/dc is the concentration dependence of the refractive index of the protein, which was found to be a constant of 0.184 mL/g with variation of 0.003 for a range of proteins.

Using this formalism, we calculated the mass per unit area of RNase A immobilized with either random or preferred orientations (Table 2). Because the ellipsometric thickness scales linearly with the amount of protein per unit surface, the ratio of the increment in the optical thickness upon binding of RNase A and RI provides the ratio of the masses of the two proteins on theses surfaces. Inspection of Table 2 leads us to three conclusions. First, the specific mass of RNase A immobilized on the surface (1.25 mg/m^2) corresponds to an areal density of ~5.5 molecules within an area 10 nm × 10 nm. We estimate native RNase A to have a dimension of approximately 4 nm × 2 nm × 1 nm by previously published crystal structures.[45] This estimation provides a surface coverage of approximately 44% of the saturation coverage based on an areal coverage of 5.5 molecules per 100 nm^2. Second, when RNase A was immobilized with a preferred orientation, the ratio of the specific masses of immobilized RI (4.25 mg/m^2) and RNase A (1.25 mg/m^2) corresponds closely to the ratio of the molecular weights of the two proteins (RI, 50 kD; RNase A, 13kD). This result is consistent with a one-to-one complex forming on the surface when RNase A is immobilized with a preferred orientation. Finally, the results presented in Table 2 suggest that the binding capacity of the SAM decorated with oriented RNase A is greater than that of the SAM presenting randomly oriented RNase A.

We further characterized these interfaces by examining the orientational behavior of liquid crystals on them. Past studies have demonstrated that the orientations assumed by liquid crystals are sensitive to the presence of proteins on interfaces when the interfaces possess nanometer-scale structure.[33−36] Here, we prepared nanostructured surfaces by oblique deposition of gold films and formed SAMs on these surfaces using procedures identical to those procedures used on uniformly deposited gold films, as reported above. These obliquely deposited gold films are composed of gold grains that possess both in-plane and out-of-plane crystallographic textures as well as anisotropic topography that can be idealized as a corrugation with an amplitude of 1−2 nm and a wavelength of 10−40 nm.[46,47] The anisotropy in the structure of the gold film guides the azimuthal orientation of liquid crystals supported on these surfaces. In addition, when decorated with SAMs, the orientations assumed by the liquid

(43) Klink, T. A.; Woycechowsky, K. J.; Taylor, K. M.; Raines, R. T. *Eur. J. Biochem.* **2000**, *267*, 566.
(44) DeFeijter, J. A.; Benjamins, J.; Veer, F. A. *Biopolymers* **1978**, *17*, 1759.
(45) Wlodawer, A.; Svensson, L. A.; Sjolin, L.; Gilliland, G. L. *Biochemistry* **1988**, *27*, 2705.
(46) Skaife, J. J.; Abbott, N. L. *Chem. Mater.* **1999**, *11*, 612.

Table 2. Ellipsometric Thickness (nm) of RNase A Immobilized with Preferred and Random Orientations, and RI Bound to Immobilized RNase A

	mixed SAMs[a]	wild-type RNase A[b]	A19C RNase A[b]	RI	BSA	RI·RNase A
path A: (oriented)	2.5 ± 0.1	2.5 ± 0.1	3 ± 0.1	4.7 ± 0.4[c]	3 ± 0.1[c]	3.3 ± 0.1[c]
	ΔTh	0 ± 0.1[d]	0.5 ± 0.1[d]	1.7 ± 0.4[e]	0 ± 0.1[e]	0.3 ± 0.1[e]
	M/A[f]	0 ± 0.25	1.25 ± 0.25	4.25 ± 1	0 ± 0.25	0.75 ± 0.25
path B: (not oriented)	2.6 ± 0.3	3.1 ± 0.1		3.5 ± 0.4[g]	3.1 ± 0.1[g]	3.2 ± 0.1[g]
	ΔTh	0.5 ± 0.1[d]		0.4 ± 0.4[h]	0 ± 0.1[h]	0.1 ± 0.1[h]
	M/A	1.25 ± 0.25		1 ± 1	0 ± 0.25	0.25 ± 0.25

[a] Mixed SAMs formed from **1** and **2**. The mole percentage of **1** in ethanol was 46%. [b] Immobilization of A19C RNase A (1 μM) or wild-type RNase A (1 μM) on mixed SAMs via path A or B (Figure 2). [c] Binding of RI, BSA, or the RI·RNase A complex to A19C RNase A immobilized on thiol-terminated SAMs. [d] Increase in ellipsometric thickness due to the binding of wild-type or A19C RNase A to the mixed SAMs. [e] Increase in ellipsometric thickness due to the binding of RI, BSA, or the RI·RNase A complex to A19C RNase A immobilized on mixed SAMs. [f] M/A (mg/m^2) is the calculated mass per unit area of protein on surface. [g] Binding of RI, BSA, or the RI·RNase A complex to wild-type RNase A immobilized on NHS-activated SAMs. [h] Increase in ellipsometric thickness due to binding of RI, BSA, or the RI·RNase A complex to wild-type RNase A immobilized on mixed SAMs.

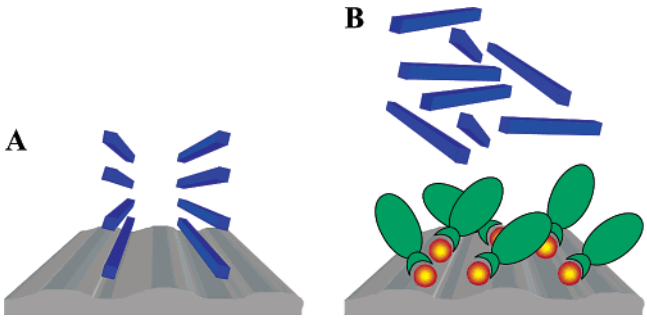

Figure 5. (A) Schematic illustration of the uniform alignment of liquid crystals on surface possessing topography that can be idealized as a nanometer-scale corrugation. The blue bar indicates the orientation of the liquid crystal. (B) Protein-binding events on the surface can mask the topography of the gold film and thus disrupt the uniform orientation of the liquid crystal.

crystal on these gold films depends on the specific functionality and orientation of the terminal groups of the SAMs.[38,47−49]

When proteins are immobilized on SAMs supported on obliquely deposited gold films, the presence of the proteins on these surfaces changes the orientation of the liquid crystal relative to that assumed by the liquid crystal in the absence of the bound protein.[33,36] Past studies have identified two possible mechanisms by which bound protein can influence the orientation of liquid crystal supported on obliquely deposited gold. First, as mentioned above, obliquely deposited gold films possess a nanometer-scale topography that can orient a liquid crystal (Figure 5A); protein bound to such a surface can prevent the uniform alignment of the liquid crystal along the corrugation of the surface (Figure 5B). Second, because the orientations of functional groups in SAMs supported on obliquely deposited gold films can also influence the orientations of liquid crystal,[49] bound proteins can mask these oriented functional groups (preventing interaction between the functional groups and liquid crystal), thus leading to a second mechanism by which protein can be reported by liquid crystal on these surfaces (Figure 5B). Both mechanisms predict that protein bound to a SAM formed on an obliquely deposited gold film will be reported as a loss in the uniform orientation of the liquid crystal.

In this work, we used gold films prepared by oblique deposition onto glass slides at an angle of 40° from the normal of the slides. We first investigated the orientational behavior of liquid crystals in contact with RNase A immobilized on SAMs supported on obliquely deposited gold films. We measured the optical appearance of a 13-μm-thick film of nematic liquid crystal 5CB sandwiched between two surfaces, both of which presented RNase A with either preferred or random orientations. In the absence of RNase A immobilized on the SAM, the liquid crystal assumed a uniform optical appearance (Figure 6A). As the sample was rotated between crossed polars, the intensity of light transmitted through the sample was strongly modulated. The uniform optical appearance and strong modulation of the brightness of the sample is consistent with a uniform planar alignment of the liquid crystal (orientation parallel to the surface). We determined that the azimuthal orientation of the planar-aligned liquid crystal was perpendicular to the direction of the incidence of gold during the deposition of the gold films.[36] In past studies, we have demonstrated that the nanometer-scale topography of obliquely deposited gold films causes the liquid crystal to assume this azimuthal orientation.[49]

The response of liquid crystal to the presence of proteins supported on obliquely deposited gold films depends on both the nanometer-scale topography of the gold films and surface area coverage of the proteins.[44] Our past studies have demonstrated that the optical appearance of a liquid crystal becomes increasingly non-uniform within a sample with increasing surface area coverage of protein. Figure 6B shows the optical appearance (crossed polars) of 5CB in contact with the SAM supporting oriented RNase A, whereas Figure 6C shows the optical texture of 5CB in contact with randomly oriented RNase A. Inspection of Figure 6B,C reveals that both samples contain large areas that have a uniform optical appearance and that upon rotation of the samples between crossed polars, optical appearance of these regions changes in a manner that is indistinguishable from the RNase-free samples shown in Figure 6A. This result indicates that the liquid crystals assume a largely (but not completely; see below for a discussion of the domains and defects in Figure 6B,C) uniform azimuthal orientation in the presence of RNase A that is the same as that assumed by the liquid crystal in the absence of RNase A on the surface. We also note that the presence of the RNase A on the surfaces does introduce domains and linear defects into the otherwise uniform orientation of the liquid crystals.

In particular, close inspection of Figure 6 reveals differences in the optical appearance of the liquid crystal in contact with the surfaces that present oriented RNase A (Figure 6B) as compared to the surfaces that present randomly oriented RNase A (Figure 6C). On surfaces that present oriented RNase A (Figure 6B), the liquid crystal possesses domains with a well-defined optical appearance (brightness) that differs from the

(47) Follonier, S.; Miller, W. J.; Abbott, N. L.; Knoesen, A. *Langmuir* **2003**, *19*, 10501.
(48) Shah, R. R.; Abbott, N. L. *J. Am. Chem. Soc.* **1999**, *121*, 11300.
(49) Gupta, V. K.; Abbott, N. L. *Science* **1997**, *276*, 1533.

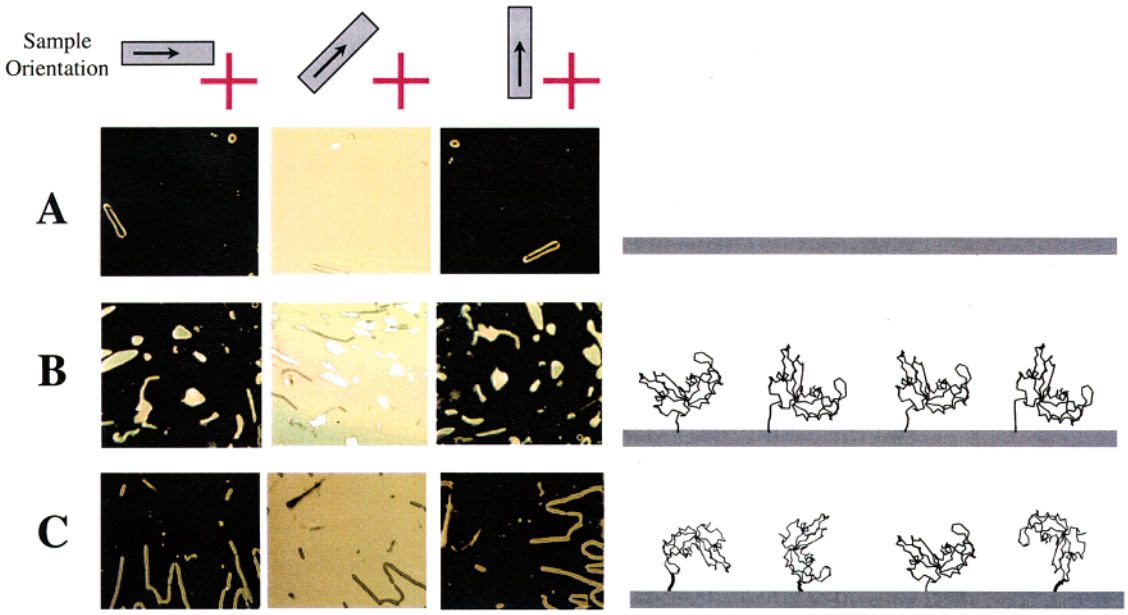

Figure 6. Optical images (crossed polarizers) of nematic 5CB sandwiched between nanostructured surfaces that support (A) mixed SAMs formed from **1** and **2**, (B) RNase A immobilized in a preferred orientation on mixed SAMs formed from **1** and **2** (Figure 2 path A), and (C) RNase A immobilized in random orientations on mixed SAMs formed from **1** and **2** (Figure 2, path B). The orientation of the sample relative to the polarizer is shown above the images of the liquid crystal. The arrow indicates the direction of gold deposition. A schematic illustration of RNase A immobilized with preferred and random orientations is shown to the right of the images of the liquid crystal.

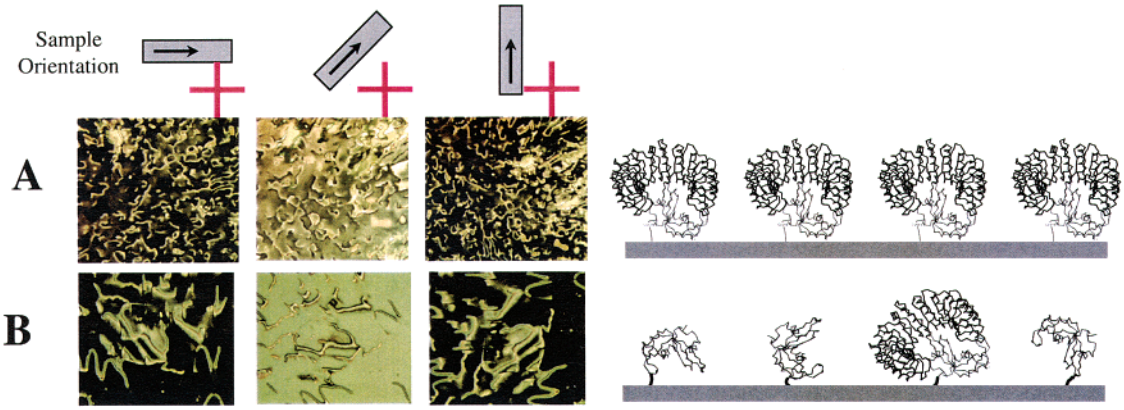

Figure 7. Use of liquid crystals to detect RI binding to RNase A immobilized on SAMs with different modes of orientation. Optical images (crossed polarizers) of nematic 5CB sandwiched between nanostructured surfaces that support (A) RI bound to preferentially oriented RNase A and (B) RI bound to randomly oriented RNase A. A schematic illustration of RI binding to RNase A immobilized with preferred and random orientations is shown to the right of the images of the liquid crystal.

appearance of the liquid crystal in the absence of RNase A. The bright domains are encircled by line defects. The coexistence of these two distinct optical domains within the liquid crystal suggests the existence of two unique orientations of the liquid crystal with different azimuthal directions on the surfaces that present oriented RNase A. In contrast, on surfaces that present randomly oriented RNase A (Figure 6C), we do not observe distinct orientational domains of liquid crystal, but rather a single domain containing line defects that do not form closed loops. Past studies have reported that the orientations of terminal functional groups of SAMs can influence the orientation liquid crystals on obliquely deposited gold films;[38,48,49] the results presented in Figure 6 suggest that the orientations of immobilized proteins may also influence the orientations of liquid crystals supported on them.

Next we measured the optical appearance of 5CB in contact with RI bound to RNase A with preferred and uniform orientations on these nanostructured surfaces. Figure 7A shows the optical appearance of 5CB in contact with RI bound to oriented RNase A, and Figure 7B shows the optical appearance of 5CB in contact with RI bound to randomly oriented RNase A. Inspection of Figure 7A reveals that 5CB assumes a *non-uniform orientation* on the surfaces with RI bound to oriented RNase A: many line defects are observed to be embedded within the liquid crystal. When compared to Figure 6B, a diminished modulation of the total intensity of the light transmitted through the sample was observed when the sample was rotated between the crossed polarizers. This result suggests that the amount of RI bound to the oriented RNase A is sufficient to largely mask the influence of the gold film and SAM on the orientation of the liquid crystal. In contrast, Figure 7B reveals a more uniform orientation of 5CB supported on the surface presenting random RNase A that was treated with RI. The optical appearance of the liquid crystal in Figure 7A, when compared to Figure 7B, indicates greater binding of RI to the oriented RNase A than that to the random RNase A on

the surface. These differences can be quantified by the standard deviation of the average luminosity of the optical texture of the liquid crystal. [36] For instance, the standard deviation of the luminosity of 5CB on the surface presenting oriented RNase A treated with RI (Figure 7A) is 75, whereas the surface presenting randomly oriented RNase A treated with RI caused the standard deviation of the luminosity of 5CB to be 45 (Figure 7B). We note here that other indices can be used to quantify the appearance of images such as those shown in Figure 7A,B. We do not yet know which index represents the optimal method of characterizing these images.

We make several observations regarding the results represented above. First, we note that the measurements of the ellipsometric thicknesses of RI bound to RNase A as well as the orientational behavior of liquid crystals are consistent with greater binding of RI to the surfaces presenting the RNase A immobilized with a preferred orientation than random orientation. Because the interfacial microenvironments of the immobilized RNase A were similar on the two surfaces, we conclude that the greater binding capacity of the oriented RI is indeed due to orientational effects and not to differences in interfacial microenvironments.

We note that a number of past studies have reported the immobilization of antibodies on surfaces in preferred orientations so that the binding ability of the antigen-binding (Fab) domains is optimized.[50] These strategies include the use of a predeposited layer of protein A or protein G that binds the Fc region of an antibody[9,10] and the use of a predeposited streptavidin layer to bind antibody (or Fab) that is conjugated with site-specific biotin.[50] When compared to immobilization schemes that do not control the orientations of immobilized antibodies (or Fab), oriented antibodies (or Fab) generally (but not always) exhibit higher binding capacity than antibodies immobilized with random orientations.[50] It is difficult, however, to assign this increase in binding capacity to the effects of orientation because the microenvironments of the surfaces that support oriented and randomly oriented antibodies are different, and thus variations in the degree of nonspecific adsorption, denaturation, and interfacial solvent structure can all contribute to differences in binding activities (as discussed above).[51,52]

In our study, we used both ellipsometry and liquid crystals to report the presence of the RI bound to the oriented RNase A. Ellipsometry reports the presence of RI as the effective optical thickness of an equivalent slab of material at the surface that possesses a refractive index of 1.46. In contrast, the orientations of liquid crystals at surfaces are sensitive to the nanometer-scale structure of the surfaces. We observed the presence of the RI bound to the RNase A to be reported as a loss of the largely uniform orientation of the liquid crystal that was observed in the absence of bound RI (Figure 6A). Because the uniform orientation of the liquid crystal observed in the absence of bound protein was caused by the structure of the obliquely deposited gold film and SAM supported on it, our observations suggest that the RI is reported by the liquid crystal because it masks the influence of the structure of the underlying gold film/SAM on the liquid crystal. This conclusion is consistent with the results of several past studies of the binding of proteins to SAMs supported on obliquely deposited gold films.[33−36]

The structure-sensitive nature of the orientational behavior of liquid crystals is also apparent in our observations of 5CB on surfaces presenting RNase A immobilized in preferred and random orientations. Whereas ellipsometry reports the effective optical thickness of the immobilized RNase A to be identical, the orientations assumed by the 5CB on the surfaces with oriented RNase A were different from the orientations of 5CB observed on the surfaces with RNase A immobilized with random orientations. In particular, we note that the liquid crystal supported on the oriented RNase A assumed two distinct orientations, whereas the liquid crystal supported on the RNase A immobilized in random orientations reported the presence of the RNase A on the surfaces as linear defects within the liquid crystal. We also note that in a past study of the immobilization of the cell-signaling protein (MEK-His-tag) on SAMs presenting nitrilotriacetic acid chelated with Ni(II), the liquid crystal also showed two distinct orientational domains on a layer of oriented MEK-His-tag supported on an obliquely deposited gold film.[52] These results, when combined, suggest that liquid crystals offer the basis of tools for reporting the organization of proteins on surfaces.

Conclusion

The principal conclusions of this article are threefold. First, by comparing two schemes that lead to the immobilization of RNase A in the same interfacial microenvironment, one which provides a controlled orientation of RNase A and another that does not, we conclude that control of the orientation of an immobilized protein receptor on a surface can have a substantial effect on the capacity of the surface to bind a protein ligand. By using surfaces that present the same amount of RNase A, our results reveal that the binding capacity of RNase A without a preferred orientation for RI is only 25% of that of RNase A presented in a controlled orientation. Because the microenvironment of the RNase A is similar in both immobilization schemes, we conclude that the binding capacity of the random RNase A is likely low because the RNase A assumes orientations in which its binding face is not accessible to RI. Second, we observed the orientations assumed by nematic 5CB on surfaces presenting RNase A to depend on the orientation of the immobilized RNase A. This result suggests that liquid crystals can be used to probe the orientations of proteins at surfaces. Third, we demonstrated that the increased binding capacity achieved by the oriented immobilization of proteins facilitated the use of liquid crystals to rapidly detect protein-binding events on surfaces.

Acknowledgment. This research was supported by funding from the Biophotonic Partnership Initiative of NSF (ECS-0086902), the Center for Nanostructured Interfaces (NSF-DMR 0079983) at the University of Wisconsin-Madison, and Grant GM 44783 (NIH to R.T.R.).

JA0398565

(50) Peluso, P.; Wilson, D. S.; Do, D.; Tran, H.; Venkatasubbaiah, M.; Quincy, D.; Heidecker, B.; Poindexter, K.; Tolani, N.; Phelan, M.; Witte, K.; Jung, L. S.; Wagner, P.; Nock, S. *Anal. Biochem.* **2003**, *312*, 113.
(51) Butler, J. E.; Ni, L.; Nessler, R.; Joshi, K. S.; Suter, M.; Rosenberg, B.; Chang, J.; Brown, W. R.; Cantarero, L. A. *J. Immunol. Methods* **1992**, *150*, 77.
(52) The orientation of the liquid crystals (5CB) on oriented MEK-His-tag is documented in Figure 7 in ref 36.